IEEE Access
Multidisciplinary | Rapid Review | Open Access Journal

Received 24 August 2022, accepted 9 September 2022, date of publication 12 September 2022, date of current version 20 September 2022.

Digital Object Identifier 10.1109/ACCESS.2022.3206369

RESEARCH ARTICLE

High-Speed Monitoring of Multidimensional Processes Using Bayesian Updates

SANGAHN KIM[1], MEHMET TURKOZ[2], AND JUNG WOO BAEK[3]
[1]Department of Business Analytics and Actuarial Science, Siena College, Loudonville, NY 12211, USA
[2]Department of Management, Marketing and Professional Sales, William Paterson University, Wayne, NJ 07470, USA
[3]Department of Industrial Engineering, Chosun University, Gwangju 61452, South Korea

Corresponding author: Jung Woo Baek (jwbaek@chosun.ac.kr)

This work was supported in part by the Chosun University 2019.

ABSTRACT The advent of modern data acquisition and computing techniques has enabled high-speed monitoring of high-dimensional processes. The short sampling interval makes the samples temporally correlated, even if there is no underlying autocorrelation among covariates. In this study, we introduce a new process monitoring scheme in a Bayesian framework. The key strategy of this study is to incorporate sequential observations into the estimation procedure for the parameters of interest to update the prior distribution. Based on the updated prior, we obtain the most appropriate estimation of the process parameters at each sampling epoch by maximizing the posterior probability. In addition, conventional statistical process control and monitoring methodologies suffer from the ''curse of dimensionality.'' The closed form of the estimate developed in this study through Bayesian updates enables the proposed method to be effective for high-dimensional process monitoring. Various simulation studies demonstrate the superiority of the proposed scheme in the high-speed monitoring of high-dimensional processes. Moreover, a few sample paths of the estimated mean in a procedure of the proposed method are illustrated to provide practitioners with insights into the monitoring and control of the process. Finally, we provide a real-life application to illustrate the proposed method.

INDEX TERMS Autocorrelated process, Bayesian update, high-dimensional process, process mean monitoring, statistical process control.

I. INTRODUCTION

Statistical process control (SPC) and monitoring techniques have been widely used to detect process changes by monitoring quality characteristics or process parameters such as mean and covariance. When there are multiple quality characteristics, a standard approach is to consider simultaneous monitoring of the mean by taking correlation into consideration in a chart statistic. Hotelling's T^2, multivariate exponentially weighted moving average (MEWMA), and multivariate CUSUM (MCUSUM) charts are good examples of simultaneous monitoring charts used for multivariate SPC (MSPC) [1], [2]. The advent of modern data acquisition and computing techniques has enabled high-speed monitoring of high-dimensional processes. Although the traditional MSPC methods can be applied to monitoring relatively high-dimensional processes, they mostly suffer from high-dimensional settings; this phenomenon is called the ''curse of dimensionality'' [3], [4].

Accordingly, many charts intended for high-dimensional processes have been developed. Principal component analysis (PCA)-based approaches are well suited for monitoring high-dimensional processes by focusing on only a few principal components (PCs) [5], [6], [7]. Although they enjoy computational efficiency, the chart performance may deteriorate depending on the shift direction, that is, they are directionally variant [8]. In addition, because the principal component is a linear combination of all variables, it is not expected to

The associate editor coordinating the review of this manuscript and approving it for publication was Yu Liu.

provide any useful information for the identification step after detecting the change, especially when only a few variables are changed.

Recently, several methods have been developed to monitor quality characteristics directly, rather than considering PCs, despite high dimensionality. One of the main assumptions of these charts is ''sparsity,'' that is, it is assumed that there are only a small set of variables causing the process change, according to the reasonably low probability of many quality characteristics changing simultaneously. Along with the assumption of sparsity, [3] and [9] developed variable selection (VS)-based procedures. They considered a two-step procedure to monitor the process: 1) identification of the possible faulty variables and 2) monitoring of the process based on the chosen variables. Reference [10] proposed a similar procedure by adopting the adaptive absolute shrinkage and selection operator (LASSO), where LASSO identifies potentially changed variables. Reference [11] combined the least angle regression to monitor both the mean and variability. Reference [12] applied forward variable selection as a pre-diagnosis and integrated it into the MCUSUM chart.

One of the advantages of VS-based methods is that they provide useful information in fault diagnosis compared to PCA-based methods because VS identifies some potentially changed variables in the first step. However, these methods mostly suffer from computational issues as the number of dimensions increases because identification is performed at every sampling point. Particularly in a high-speed monitoring environment, this computational issue makes the chart impractical. In addition, the charts may not perform well if the VS procedure incorrectly identifies the changed variables owing to the small size of the shift [8]. To overcome the issues of VS-based methods, [8] applied L_2 regularization—or ridge regularization—in the likelihood function. They developed a theoretical procedure and evaluated the average run length (ARL) performance using the approximate probability distribution of the chart statistics based on the closed form of the estimate of the mean at each sampling point. This method has proven its usefulness in high-dimensional and high-speed monitoring processes in that the closed form of the estimate significantly improves computational concern. However, the ridge regularization has different shrinkage rates depending on the covariance structure, which results in the chart being directionally variant. Although [8] determined the theoretical performance, the directional variant property of the chart makes it difficult to detect a change when it occurs in certain directions.

In this article, we propose a novel monitoring procedure developed under a Bayesian framework for high-speed monitoring processes in relatively high-dimensional processes. In a high-speed monitoring environment, it is essential to assume that the observations may be autocorrelated, although the nominal process parameters are assumed to be constant over time. This assumption makes more sense in an out-of-control situation. It is reasonable that a process changes slightly over time after the shift occurs, which is not necessarily a sudden jump. For example, in a milling machining process, the milling tool starts oscillating gradually as it wears out, resulting in an oscillating pattern of the out-of-control signal [8]. Another example can be found in chemical processes. In the literature of the Tennessee Eastman Industrial Challenge Problem (TE problem [13]), it is shown that most of the measurements show insignificant autocorrelation when the process is operating in normal mode. However, the system shows severe dynamic behavior when disturbances are added [14]. Figure 1 illustrates the in-control data pattern of one of the variables in the TE process, reactor coolant temperature, and Figures 2 and 3 show the out-of-control situation after the disturbances are added. Figures 1–3 demonstrate that the mean of the process in the out-of-control state is patterned dynamically by time, while the process has a stable constant mean in a normal operating state.

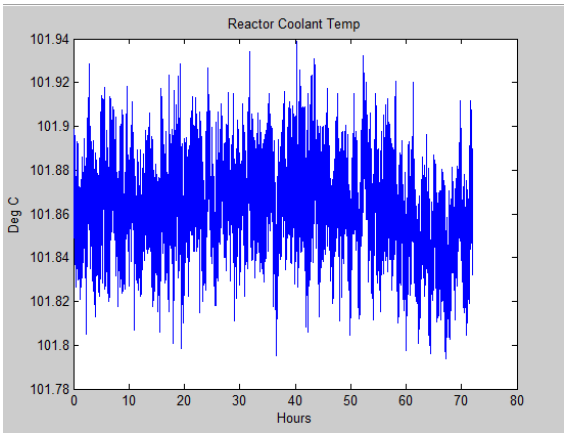

FIGURE 1. In-control signal of a variable (reactor coolant temperature) in TE process.

The proposed method considers the probability distribution of the process mean $\boldsymbol{\mu}_t$ in a Bayesian framework. In particular, $\boldsymbol{\mu}_t$ can be observed on a stochastic basis and determined through the path $\boldsymbol{\mu}_{t-1}, \boldsymbol{\mu}_{t-2}, \ldots, \boldsymbol{\mu}_1$, that is, the Bayesian theorem updates the posterior distribution of $\boldsymbol{\mu}_t$ sequentially. The rationale behind the underlying dynamics is that the current process mean is essentially associated with previous means in a high-speed monitoring environment. This suffices considering the possible autocorrelation in a high-speed sampling process, and therefore, the model would explain the out-of-control dynamics more appropriately, although the in-control process mean is assumed to be constant over time. In addition, we focus on the detection of the process mean change, while the process variability remains unchanged.

Another main challenge is to overcome the computational issue in multi-dimensional processes without dimension reduction, which requires extensive computational efforts as the dimension (p) increases. The recently developed VS-based methods that adopt penalized likelihood demand a large amount of computation as p increases.

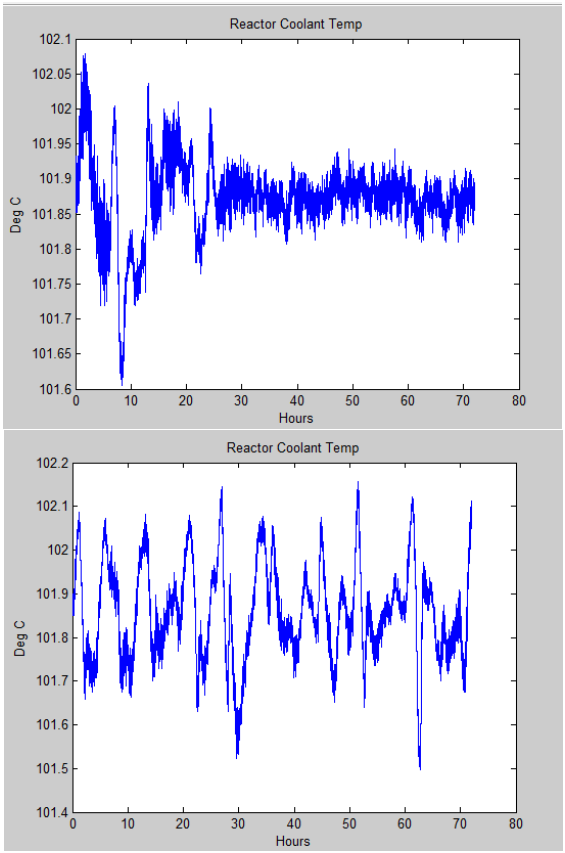

FIGURE 2. Dynamic pattern of the out-of-control situation in reactor coolant temperature.

For example, [10] adopted L_1-based regularization (LASSO penalty), and [3] and [9] utilized forward variable selection for pre-diagnosis to solve L_0-based regularization. In general, solving L_0 penalized likelihood requires extensive computation. For example, among decomposition procedures, the MTY decomposition theoretically sounds similar to the best subset selection [15]. However, it must examine $p!$ decompositions, so it is impractical in a high-dimensional process. Some step-down procedures have been proposed to overcome the computational issue in a high-dimensional process, such as the adaptive step-down (ASD) method, which requires only $O(p^2)$ calculations [16]. However, even though ASD significantly reduces the computational complexity, it is still inappropriate when the procedure is running sequentially over the sampling period. Similarly, although some algorithms and VS techniques such as forward and stepwise VS are computationally efficient, they are inappropriate to be incorporated into process monitoring as a pre-diagnosis procedure, especially in high-speed monitoring processes.

The proposed method enjoys the computational benefit in that the process mean at a sampling point, t, that is, $\hat{\boldsymbol{\mu}}_t$ is obtained theoretically as a closed form via Bayesian updates. The closed form of the estimate of the mean makes process monitoring very effective when samples are taken frequently in multi-dimensional processes, compared to VS-based methods, which demand heavy computation. One may argue that VS-based methods provide diagnostic information about faulty variables, although they are computationally inefficient. Indeed, the proposed method does not explicitly identify faulty variables, unlike VS-based methods. However, the method provides meaningful probabilities indicating which variables can potentially be out of control. This would be attractive for practitioners to anticipate how the process proceeds at the next sampling point.

The Bayesian framework has paid attention and been widely used in statistical control of processes where the use of Bayesian methods takes the advantage of the process knowledge incorporated into the methodology through the prior distributions. Many of them focus on the optimality of the chart design to determine control policy [17], [18], [19], [20], [21]. In addition, the Bayesian theory has also been used to determine the time to signal of fault [22]. However, quite a few Bayesian methods have been studied in process monitoring, most of which are univariate process monitoring with theoretical and practical progress [23], [24], [25], [26], [27], [28]. Reference [29] mentioned that few researchers have developed the extension to the multivariate setting. Reference [30] developed the change point estimation procedure in Bayesian context given that an out-of-control signal was raised. Reference [31] developed a Bayesian hierarchical model to determine the means and directions of the shifts with a given suspected out-of-control sample. Reference [32] applied dynamic Bayesian estimation to detect machine failures in a discrete multivariate situation. Recently, [33] applied Bayesian sequential update when the assignable causes are sparse. This paper proposes a Bayesian method to monitor the process mean in multivariate online processes and shows the advantage of using updated prior distribution in high-dimensional process monitoring.

The proposed method provides simplicity in using Bayesian updates in process monitoring and opens further investigation in statistical process monitoring. The novelty of the work can be summarized into two major aspects. First, the updated parameters at every sampling point in a high-speed sampling process enabled the monitoring statistic to be more efficient than conventional control charts. Few studies have been conducted in this circumstance. Although [33] applied the Bayesian sequential update in high-dimensional processes, it assumed sparsity in the out-of-control process. The proposed model is developed without sparsity assumption, thereby generalizing [33]. Second, the proposed method is computationally inexpensive. The closed-form estimate developed in later sections enables effective in high-dimensional process monitoring in contrast to many previous studies that are computationally expensive and hard to apply in practice.

The remainder of this paper is organized as follows. In the next section, we describe our proposed method based on a Bayesian update from the perspective of process monitoring and control. In Section 3, we compare the proposed

procedure with other existing process monitoring methods through various simulations. In Section 4, we discuss the posterior probability distribution of the process mean and present a predictive analysis that would be useful in monitoring and diagnosing faults. Section 5 illustrates the proposed method with a real-life example, followed by concluding remarks and a discussion of future research in Section 6.

II. METHODOLOGY

A. ESTIMATING PROCESS MEAN IN BAYESIAN FRAMEWORK

Let a single measurable observation $\mathbf{x}_t$ be the p-dimensional vector and $\boldsymbol{\mu}_t$ be the unknown process parameter, which is the mean of the process. We assume that only one observation is taken at every sampling epoch, and the interval of the samples is relatively short, owing to the advent of modern data processing and acquisition technology. Then, the linear generative model is defined statistically as

$$\mathbf{x}_t = \mathbf{Z}_t \boldsymbol{\mu}_t + \boldsymbol{\varepsilon}_t \tag{1}$$

where $\mathbf{Z}_t$ is a basis matrix to convert the unobservable mean to a measurable observation, and $\boldsymbol{\varepsilon}_t$ represents the randomness that has zero mean with a covariance $\boldsymbol{\Sigma}$. Because the variability of the process measurements is represented by $\boldsymbol{\varepsilon}_t$ statistically, we assume that the variability remains unchanged over time, and $\boldsymbol{\varepsilon}_t \sim N(\mathbf{0}, \boldsymbol{\Sigma})$.

The unknown parameter $\boldsymbol{\mu}_t$ can be stochastically defined in dynamics to incorporate the possible autocorrelation in a high-speed monitoring process as follows:

$$\boldsymbol{\mu}_t = \mathbf{T}_t \boldsymbol{\mu}_{t-1} + \mathbf{R}_t \boldsymbol{\eta}_t \tag{2}$$

where the matrices $\mathbf{T}_t$ and $\mathbf{R}_t$ are the parameters used to model the autocorrelation and moving errors [34]. $\boldsymbol{\eta}_t$ is the randomization term in the state of the mean and follows $N(\mathbf{0}, \mathbf{Q})$. In the context of SPC, we consider the randomness to be serially independent and independent of $\boldsymbol{\varepsilon}_t$. We also assume that the errors are identically distributed over the sampling time, which makes sense to describe the complete randomness of the in-control process. Some literature on monitoring autocorrelated measurements attempts to estimate the autocorrelation parameters first [33], [34], [35], [36], [37], [38], [39] or at least assumes the autocorrelation parameters to be known, that is, the matrices $\mathbf{T}$ and $\mathbf{R}$ are estimated or given. Throughout the paper, we assume Markovian state dynamics with the identity matrices for $\mathbf{T}$ and $\mathbf{R}$ to generalize the model under the assumption that the process parameter is unknown and non-measurable.

We now incorporate the Bayesian probability into the model. The strategy for increasing the sensitivity of monitoring is to directly monitor the process mean through the estimates of the parameters rather than monitoring the measurements that imply the mean. To obtain the best estimate of $\boldsymbol{\mu}_t$, that is, $\hat{\boldsymbol{\mu}}_t$, we consider the posterior distribution of $\boldsymbol{\mu}_t$ given all past observations and previous means and try to maximize the posterior probability. Let $P\left(\boldsymbol{\mu}_t \mid \boldsymbol{\mu}_{t-1}, \boldsymbol{\mu}_{t-2}, \ldots, \boldsymbol{\mu}_1, \mathbf{x}_t, \mathbf{x}_{t-1}, \ldots, \mathbf{x}_1\right)$ be the posterior distribution of $\boldsymbol{\mu}_t$. Using the Bayesian rule for conditional distribution, we can obtain the probability as

$$P\left(\boldsymbol{\mu}_t \mid \boldsymbol{\mu}_{t-1}, \boldsymbol{\mu}_{t-2}, \ldots, \boldsymbol{\mu}_1, \mathbf{x}_t, \mathbf{x}_{t-1}, \ldots, \mathbf{x}_1\right) = \frac{P\left(\boldsymbol{\mu}_t, \boldsymbol{\mu}_{t-1}, \ldots, \boldsymbol{\mu}_1, \mathbf{x}_t, \mathbf{x}_{t-1}, \ldots, \mathbf{x}_1\right)}{P\left(\boldsymbol{\mu}_{t-1}, \boldsymbol{\mu}_{t-2}, \ldots, \boldsymbol{\mu}_1, \mathbf{x}_t, \mathbf{x}_{t-1}, \ldots, \mathbf{x}_1\right)}. \tag{3}$$

The joint distribution $P\left(\boldsymbol{\mu}_t, \boldsymbol{\mu}_{t-1}, \ldots, \boldsymbol{\mu}_1, \mathbf{x}_t, \mathbf{x}_{t-1}, \ldots, \mathbf{x}_1\right)$ can be obtained recursively as

$$\begin{aligned} &P\left(\boldsymbol{\mu}_t, \boldsymbol{\mu}_{t-1}, \ldots, \boldsymbol{\mu}_1, \mathbf{x}_t, \mathbf{x}_{t-1}, \ldots, \mathbf{x}_1\right) \\ &\quad = P\left(\boldsymbol{\mu}_t, \ldots, \boldsymbol{\mu}_1\right) \times \prod_{i=1}^{t} \\ &\qquad \times P\left(\mathbf{x}_i \mid \mathbf{x}_{i-1}, \ldots, \mathbf{x}_1, \boldsymbol{\mu}_i, \boldsymbol{\mu}_{i-1}, \ldots, \boldsymbol{\mu}_1\right), \end{aligned} \tag{4}$$

where $P\left(\boldsymbol{\mu}_t, \ldots, \boldsymbol{\mu}_1\right)$ can also be obtained similarly as

$$P\left(\boldsymbol{\mu}_t, \ldots, \boldsymbol{\mu}_1\right) = P\left(\boldsymbol{\mu}_0\right) \prod_{i=1}^{t} P\left(\boldsymbol{\mu}_i \mid \boldsymbol{\mu}_{i-1}, \boldsymbol{\mu}_{i-2}, \ldots, \boldsymbol{\mu}_1\right) \tag{5}$$

using a Markovian property. By plugging (5) into (4), we obtain the joint probability as

$$\begin{aligned} &P\left(\boldsymbol{\mu}_t, \boldsymbol{\mu}_{t-1}, \ldots, \boldsymbol{\mu}_1, \mathbf{x}_t, \mathbf{x}_{t-1}, \ldots, \mathbf{x}_1\right) \\ &\quad = P\left(\boldsymbol{\mu}_0\right) \prod_{i=1}^{t} P\left(\boldsymbol{\mu}_i \mid \boldsymbol{\mu}_{i-1}, \boldsymbol{\mu}_{i-2}, \ldots, \boldsymbol{\mu}_1\right) \\ &\qquad \times P\left(\mathbf{x}_i \mid \mathbf{x}_{i-1}, \ldots, \mathbf{x}_1, \boldsymbol{\mu}_i, \ldots, \boldsymbol{\mu}_1\right) \end{aligned} \tag{6}$$

Then, the posterior distribution in (3) can be derived as

$$\begin{aligned} &P\left(\boldsymbol{\mu}_t \mid \boldsymbol{\mu}_{t-1}, \boldsymbol{\mu}_{t-2}, \ldots, \boldsymbol{\mu}_1, \mathbf{x}_t, \mathbf{x}_{t-1}, \ldots, \mathbf{x}_1\right) \\ &\quad \propto P\left(\mathbf{x}_t \mid \mathbf{x}_{t-1}, \ldots, \mathbf{x}_1, \boldsymbol{\mu}_t, \boldsymbol{\mu}_{t-1}, \ldots, \boldsymbol{\mu}_1\right) \\ &\qquad \cdot P\left(\boldsymbol{\mu}_t \mid \boldsymbol{\mu}_{t-1}, \boldsymbol{\mu}_{t-2}, \ldots, \boldsymbol{\mu}_1\right) \end{aligned} \tag{7}$$

When the observations are independent and are only determined by the current mean $\boldsymbol{\mu}_t$, (7) can be written as

$$\begin{aligned} &P\left(\boldsymbol{\mu}_t \mid \boldsymbol{\mu}_{t-1}, \boldsymbol{\mu}_{t-2}, \ldots, \boldsymbol{\mu}_1, \mathbf{x}_t, \mathbf{x}_{t-1}, \ldots, \mathbf{x}_1\right) \\ &\quad \propto P\left(\mathbf{x}_t \mid \boldsymbol{\mu}_t\right) P\left(\boldsymbol{\mu}_t \mid \boldsymbol{\mu}_{t-1}, \boldsymbol{\mu}_{t-2}, \ldots, \boldsymbol{\mu}_1\right) \end{aligned} \tag{8}$$

The result from (8) provides important findings for the Bayesian framework. The first term $P\left(\mathbf{x}_t \mid \boldsymbol{\mu}_t\right)$ is the likelihood probability, similar to the classical decomposition of the Bayesian posterior distribution. However, the second term is not a prior probability, $P(\boldsymbol{\mu})$, but a prior probability given previous means. This is a significant finding that can be interpreted as an updated prior distribution. By letting $P(\boldsymbol{\mu})$ be a probability density function of $\boldsymbol{\mu}$ as a prior distribution, it can be seen as a conditional distribution given all previous means by incorporating Markovian state dynamics as

$$P\left(\boldsymbol{\mu}_t \mid \boldsymbol{\mu}_{t-1}, \boldsymbol{\mu}_{t-2}, \ldots, \boldsymbol{\mu}_1\right) = P\left(\boldsymbol{\mu}_t \mid \boldsymbol{\mu}_{t-1}\right), \quad t = 1, 2, \ldots$$

and the distribution is $P\left(\boldsymbol{\mu}_0\right)$ at time $t = 0$.

In fact, this can be observed in Gaussian Kalman update as well. Let the location and scale parameters be $\boldsymbol{\theta}$ and $\mathbf{K}$, respectively. As shown in [33] and [34], these two parameters

are determined recursively at every sampling epoch. More importantly with the Gaussian error distribution, not only the location parameter but also the scale parameter is updated clearly as a closed form (see [34] for detailed derivation of $\boldsymbol{\theta}_t$ and $\mathbf{K}_t$).

Thus, we can conclude that the posterior probability is proportional to the likelihood and updated prior probabilities in the Bayesian context.

Now, we obtain the most probable process mean, $\hat{\boldsymbol{\mu}}_t$ by maximizing the posterior probability (MAP) as

$$\hat{\boldsymbol{\mu}}_t = \arg\max_{\boldsymbol{\mu}_t} P\left(\boldsymbol{\mu}_t \mid \mathbf{x}_t\right) = \arg\max_{\boldsymbol{\mu}_t} P\left(\mathbf{x}_t \mid \boldsymbol{\mu}_t\right) P\left(\boldsymbol{\mu}_t \mid \boldsymbol{\mu}_{t-1}\right) \tag{9}$$

With the Gaussian errors for $\boldsymbol{\eta}$ and $\boldsymbol{\varepsilon}$, the estimate is identical to

$$\hat{\boldsymbol{\mu}}_t = \arg\min_{\boldsymbol{\mu}_t} \left\{ \left\| \mathbf{x}_t - \mathbf{Z}_t \boldsymbol{\mu}_t \right\|^2_{2,\boldsymbol{\Sigma}} + \left\| \boldsymbol{\mu}_t - \mathbf{T}_t \hat{\boldsymbol{\mu}}_t \right\|^2_{2,\mathbf{P}_{t|t-1}+\mathbf{Q}} \right\} \tag{10}$$

where $\|\mathbf{x}\|^2_{2,\mathbf{A}}$ represents $\mathbf{x}^T\mathbf{A}^{-1}\mathbf{x}$. We set the predictive mean to be determined using the previous estimate. Then, the minimization problem in (10) can be solved analytically by setting the derivative with respect to $\mathbf{x}_t$ equal to zero, that is, $\frac{\partial}{\partial \mathbf{x}_t} = 0$. The solution of (10) has the following recursive form:

$$\hat{\boldsymbol{\mu}}_t = \hat{\boldsymbol{\mu}}_{t-1} + \mathbf{P}_{t|t-1}\mathbf{Z}_t^H \left[\mathbf{Q} + \mathbf{Z}_t \mathbf{P}_{t|t-1} \mathbf{Z}_t^H\right]^{-1} \left(\mathbf{x}_t - \hat{\boldsymbol{\mu}}_{t-1}\right) \tag{11}$$

which is the same solution obtained from a Gaussian Kalman filter. It is interesting to note that the Kalman filter attempts to find the most likely cause of the measurement given the approximation made by a flawed estimation and has a solution identical to that of the Bayesian approach [33], [34], [41].

B. PROPOSED CHART

Consider the hypotheses $H_0 : \boldsymbol{\mu} = \boldsymbol{\mu}_0$ vs. $H_1 : \boldsymbol{\mu} = \boldsymbol{\mu}_1$ where $\boldsymbol{\mu}_0$ is an in-control mean and $\boldsymbol{\mu}_1$ is an out-of-control mean that can be a function of sampling time but is not equal to $\boldsymbol{\mu}_0$. In classical SPC literature, the testing hypothesis exploits the measurement $\mathbf{x}_t$ and considers it to be the best unbiased estimator of $\boldsymbol{\mu}_t$ with a single observation available. Then, the monitoring statistic from the likelihood ratio test is the same as Hotelling's T^2 statistic, that is, $Q = \left(\mathbf{x}_t - \boldsymbol{\mu}_0\right)^T \boldsymbol{\Sigma}_0^{-1}(\mathbf{x}_t - \boldsymbol{\mu}_0)$. Here, the measurement $\mathbf{x}_t$ can be interpreted as an estimate of the mean at time t. Therefore, the strategy of the proposed method is to use the better estimated parameters in the state dynamics, that is, $\hat{\boldsymbol{\mu}}_t$ and $\mathbf{P}_{t|t}$. With the assumption of Gaussian error distributions, $\hat{\boldsymbol{\mu}}_t$ also follows a Gaussian distribution with covariance $\mathbf{P}_{t|t}$. Therefore, we construct the monitoring statistic of the proposed chart as

$$Q = \left(\hat{\boldsymbol{\mu}}_t - \boldsymbol{\mu}_0\right)^T \mathbf{P}_{t|t}^{-1} \left(\hat{\boldsymbol{\mu}}_t - \boldsymbol{\mu}_0\right). \tag{12}$$

The propagated estimate of the covariance matrix $\mathbf{P}_{t|t}$ is derived by $E[\hat{\boldsymbol{\mu}}_t \hat{\boldsymbol{\mu}}_t^H]$ and also has a solution with a recursive form:

$$\begin{aligned} \mathbf{P}_{t|t} &= E\left[\hat{\boldsymbol{\mu}}_t \hat{\boldsymbol{\mu}}_t^H\right] \\ &= \mathbf{P}_{t|t-1} - \mathbf{P}_{t|t-1}\mathbf{Z}_t^H \left[\mathbf{Q} + \mathbf{Z}_t \mathbf{P}_{t|t-1} \mathbf{Z}_t^H\right]^{-1} \mathbf{Z}_t \mathbf{P}_{t|t-1} \end{aligned} \tag{13}$$

In (12), the exact covariance matrix is used to monitor the process. However, with the assumption of stable variability over time in a steady-state process, it is reasonable to assume that the covariance of the mean is also stable. Thus, we replace $\mathbf{P}_{t|t}$ with an asymptotic covariance $\mathbf{P}_\infty$, given below:

$$\mathbf{P}_\infty = \mathbf{T}\left(\mathbf{P}_\infty - \mathbf{P}_\infty \mathbf{Z}^H \left[\mathbf{Q} + \mathbf{Z}\mathbf{P}_\infty \mathbf{Z}^H\right]^{-1} \mathbf{Z}\mathbf{P}_\infty\right)\mathbf{T}^H + \mathbf{R} \tag{14}$$

The equations (13) and (14) are called the discrete-time algebraic Riccati equation, which can be numerically solved—this can be done by using the idare function in MATLAB version R2019b or later. Finally, the chart triggers an alarm when $Q = \left(\hat{\boldsymbol{\mu}}_t - \boldsymbol{\mu}_0\right)^T \mathbf{P}_\infty^{-1} \left(\hat{\boldsymbol{\mu}}_t - \boldsymbol{\mu}_0\right) > c$, where c is a predetermined threshold associated with a significance level and is obtained through Monte Carlo simulations. We name our proposed chart the Bayesian SPC (BSPC).

III. PERFORMANCE ANALYSIS THROUGH NUMERICAL STUDIES

A. AVERAGE RUN LENGTH

In this section, we report various simulations to demonstrate the superiority of the proposed chart. The performance of the control charts is commonly measured by the average run length (ARL), which is the time to detect the out-of-control process. The ARLs in the in-control and out-of-control states, denoted as ARL0 and ARL1, respectively, are calculated as follows:

$$\mathrm{ARL}_0 = \frac{1}{P\left(Q > c \mid \boldsymbol{\mu}_0\right)}, \quad \mathrm{ARL}_1 = \frac{1}{P\left(Q > c \mid \boldsymbol{\mu}_1\right)}.$$

We set ARL_0 to 200, which is equivalent to the significance level of the test being set as 0.005. The basis matrix $\mathbf{Z}_t$ is considered to be an identity matrix in that the measurement $\mathbf{x}_t$ is observed directly from the mean $\boldsymbol{\mu}_t$. One of the utilizations of the basis matrix is to determine it as a square root of $\boldsymbol{\Sigma}$, which is an orthogonal transformation of the measurement $\mathbf{x}_t$. This will be useful when a practitioner considers the principal components to monitor the process. The parameter matrices $\mathbf{T}_t$ and $\mathbf{R}_t$ are also set as identity matrices, as stated in the previous section. Lastly, the covariance matrices of errors $\boldsymbol{\eta}$ and $\boldsymbol{\varepsilon}$ are assumed to be identical. In fact, the error distributions are not necessarily identical. Specifically, the covariance of the mean can be in any form based on engineering knowledge or the structure of the process dynamics. However, in this study, we let $\mathbf{Q} \equiv \boldsymbol{\Sigma}$ to represent that the variability of the measurement is identical to that of the underlying mean. Moreover, we consider the covariance matrix $\boldsymbol{\Sigma}$ as a correlation matrix without loss of generality and assume

strong correlations. In addition, we consider the spatial relationships of the variables in $\boldsymbol{\Sigma}$. The correlation coefficients $\rho\left(x_{ij}, x_{kl}\right) = r^{\sqrt{(i-k)^2+(j-l)^2}}$ for $i, k = 1, 2, \ldots, p_X$ and $j, l = 1, 2, \ldots, p_Y$, where p_X and p_Y represent the horizontal and vertical dimensions for one frame of spatial data information. Thus, $p_X \times p_Y = p$, and $0 < r < 1$ [8], [42], [43], [44]. We consider a strong correlation by setting $r = 0.9$.

In the first simulation, we compared BSPC with a traditional Hotelling T^2. The shift size δ was considered through a noncentrality parameter, that is, $\delta^2 = \left(\boldsymbol{\mu}_1 - \boldsymbol{\mu}_0\right)^T \boldsymbol{\Sigma}^{-1}(\boldsymbol{\mu}_1 - \boldsymbol{\mu}_0)$. Without loss of generality, we assume $\boldsymbol{\mu}_0 = \mathbf{0}$. Table 1 presents the ARL1 results with the dimensions $p = 10, 20$, and 50 according to the different sizes of δ. As shown in Table 1, there was a significant improvement in ARL1 compared to Hotelling's T^2 chart.

TABLE 1. ARL1 comparison of BSPC with Hotelling's T^2.

$\delta \setminus p$	$p = 10$		$p = 20$		$p = 50$	
	T^2	BSPC	T^2	BSPC	T^2	BSPC
0.5	132.28	89.06	151.29	113.26	169.33	138.70
1.0	50.78	20.71	73.60	31.77	106.37	56.81
1.5	17.14	6.39	28.04	9.73	54.07	19.42
2.0	6.42	3.13	11.29	4.28	24.69	7.56
2.5	2.96	1.98	4.90	2.52	11.15	3.93
3.0	1.72	1.48	2.54	1.81	5.38	2.54
3.5	1.25	1.21	1.60	1.41	2.92	1.90
4.0	1.07	1.07	1.25	1.19	1.84	1.52
4.5	1.02	1.02	1.07	1.06	1.35	1.28
5.0	1.00	1.00	1.01	1.02	1.13	1.12

Typically, ARL_1 increases as the dimension increases, and as the shift size decreases. Recently, a few methodologies have been developed for monitoring high-dimensional processes with the assumption of sparsity. Therefore, in the next experiment, we compared the performance of BSPC in sparse settings in $\boldsymbol{\mu}_1$ with VSMSPC, which was proposed by [3]. Let p_0 be the number of changed variables.

According to the sparsity setting, we set $p_0 = 2$, that is, $\|\boldsymbol{\mu}_1\|_0 = 2$ and $\boldsymbol{\mu}_1 = [\delta, \delta, 0, 0, \ldots, 0]^T$. Note that δ is an additive shift in this case rather than a noncentrality parameter. VSMSPC requires a parameter to determine the number of selected variables, denoting it as s. With $p_0 = 2$, the overall best parameter was obtained as $s = 2$. For the best performance, we chose $s = 2$. Table 2 shows the ARL_1 performance as p changes. A few findings were observed in this study. First, VSMSPC underperforms compared to T^2 when the shift size is small, whereas BSPC outperforms VSMSPC and T^2. This is because the VSMSPC chart may not detect the out-of-control signal when the shift size is small because of the possible misidentification of the faulty variables at the diagnosis step. In the same sense, VSMSPC performs slightly better than the other charts when the shift size is large. However, even in this large shift case, the performance of BSPC is competitive.

When a small shift size is expected in a process, practitioners may consider EWMA for the measurement instead of $\mathbf{x}_t$, that is, an EWMA vector $\mathbf{z}_t = (1 - \lambda)\,\mathbf{z}_{t-1} + \lambda \mathbf{x}_t$ [2], [45]. A CUSUM may also be the one of candidates for detecting the small change in the process, but herein, we only apply EWMA for simplicity. Based on the asymptotic Gaussian distribution of $\hat{\boldsymbol{\mu}}_t$, we can derive the posterior distribution in the manner described in Section 2. Then, the monitoring statistic becomes $Q_{\mathbf{z}} = \left(\hat{\boldsymbol{\mu}}_{\mathbf{z},t} - \boldsymbol{\mu}_{\mathbf{z},0}\right)^T \mathbf{P}_{\mathbf{z},\infty}^{-1} \left(\hat{\boldsymbol{\mu}}_{\mathbf{z},t} - \boldsymbol{\mu}_{\mathbf{z},0}\right)$, where the subscript $\mathbf{z}$ represents EWMA. The EWMA version of BSPC is referred to as multivariate Bayesian EWMA (BEWMA) throughout the paper. For the comparison models, we consider MEWMA and VSMEWMA, which are the EWMA versions of T^2 and VSMSPC. The shift δ is determined as an additive shift, and we only consider $\delta = 0.2, 0.4, 0.6, 0.8$, and 1 because EWMA-based control charts focus on small shift sizes. The EWMA parameter λ is set to 0.2. In addition, we consider the steady-state process in which the shift occurs after the process is stabilized. To implement the steady-state process, we generated the out-of-control signals after 100 samplings and ignored any false alarms during the 100 samplings.

Tables 3 and 4 show the results of two different out-of-control scenarios in terms of sparsity. In that VSMEWMA pursues high-dimensional process monitoring with sparsity, we set the same sparsity as that in the previous experiment, that is, $p_0 = 2$ for Table 3. In the Table 4 scenario, we set $p_0 = 8$, which is less sparse than the value used for Table 3. For both experiments, we set $s = 2$, which is the overall best parameter for VSMEWMA. Table 3 presents the same pattern of results as in Table 2. The proposed BEWMA outperforms MEWMA for all shift sizes. In extreme cases such as $\delta = 0.2$, BEWMA outperforms VSMEWMA because the performance of VS-based charts is expected to decrease when the shift size is small owing to the possible misidentification of the potentially changed variables. However, as the shift size increases, BEWMA performs similarly to VSMEWMA and starts comparatively underperforming. In Table 4, with a less sparse setup, we can see that the proposed BEWMA outperforms MEWMA and VSMEWMA in all shift scenarios. In addition to the case with $p_0 = 8$, we can conjecture that the performance of VSMEWMA deteriorates as p_0 increases because the chart selects only two variables ($s = 2$) and loses too much information about the process, whereas BEWMA still performs well because the chart incorporates the probabilities of all variables into the monitoring process.

In the next experiments, we attempted various out-of-control scenarios with varying shift directions. This is worth checking because most of the high-dimensional aiming charts that have been recently proposed are directionally variant, that is, the performance differs according to the shift direction. Recently, [8] proposed a ridge-regularization-based chart, showed the performance in various shift directions, and calculated the relative mean index (RMI) to measure the

TABLE 2. ARL1 comparison of BSPC with VSMSPC and Hotelling's T^2.

$\delta \setminus p$	$p = 10$			$p = 20$			$p = 50$		
	T^2	VSMSPC	BSPC	T^2	VSMSPC	BSPC	T^2	VSMSPC	BSPC
0.5	132.28	132.73	88.94	151.29	156.43	112.07	169.33	176.24	136.40
1.0	50.78	49.74	20.50	73.60	72.70	31.47	106.37	107.74	56.61
1.5	17.14	15.92	6.40	28.04	24.57	9.74	54.07	42.02	19.43
2.0	6.42	5.74	3.12	11.29	8.48	4.27	24.69	14	7.57
2.5	2.96	2.64	1.98	4.90	3.57	2.51	11.15	5.23	3.92
3.0	1.72	1.56	1.47	2.54	1.90	1.80	5.38	2.47	2.54
3.5	1.25	1.18	1.21	1.60	1.29	1.42	2.92	1.51	1.89
4.0	1.07	1.04	1.07	1.25	1.08	1.18	1.84	1.16	1.51
4.5	1.02	1.01	1.02	1.07	1.02	1.06	1.35	1.04	1.28
5.0	1.00	1.00	1.00	1.01	1.00	1.02	1.13	1.01	1.12

TABLE 3. ARL1 comparison of BEWMA with VSMEWMA and MEWMA when $p_0 = 2$.

$\delta \setminus p$	$p = 25$			$p = 50$		
	MEWMA	VSMEWMA	BEWMA	MEWMA	VSMEWMA	BEWMA
0.2	152.52	160.97	146.77	164.13	170.98	162.46
0.4	78.62	78.24	71.14	100.2	100.5	93.69
0.6	37.83	33.62	33.77	53.14	43.39	48.20
0.8	20.71	16.98	18.21	29.24	20.64	25.77
1.0	13.15	10.56	11.72	18.19	12.3	15.68

TABLE 4. ARL1 comparison of BEWMA with VSMEWMA and MEWMA when $p_0 = 8$.

$\delta \setminus p$	$p = 25$			$p = 50$		
	MEWMA	VSMEWMA	BEWMA	MEWMA	VSMEWMA	BEWMA
0.2	78.00	96.86	72.05	99.89	120.75	94.91
0.4	20.82	26.57	18.26	29.10	37.60	25.86
0.6	9.61	11.58	8.38	12.66	14.54	10.99
0.8	6.24	6.93	5.54	7.82	8.35	6.81
1.0	4.68	5.04	4.23	5.81	5.79	5.04

performance, which is given as

$$\text{RMI} = \frac{1}{N}\sum_{i=1}^{N}\frac{\text{ARL}_{\boldsymbol{\mu}_i}(X) - \text{ARL}^*_{\boldsymbol{\mu}_\mathbf{i}}}{\text{ARL}^*_{\boldsymbol{\mu}_\mathbf{i}}}$$

where N is the number of out-of-control scenarios, $\text{ARL}_{\boldsymbol{\mu}_i}(X)$ is the ARL1 value of the given chart X, and $\text{ARL}^*_{\boldsymbol{\mu}_\mathbf{i}}$ is the smallest ARL1 among the charts under shift $\boldsymbol{\mu}_i$. Thus, RMI measures the relative performance among the considered scenarios and is useful for comparing directionally variant charts under various scenarios. We now compare the performance of BSPC, VSMSPC, RMSPC [8], and T^2. It is also noteworthy that the pattern of the performance would be similar if we consider EWMA for all charts, that is, BEWMA, VSMEWMA, RMEWMA, and MEWMA. Table 5 shows the ARL1 with the relative index in parentheses, and at the bottom of the table, the RMI is shown. Based on the nature of the index, a lower RMI value represents better performance. The experiment was conducted under the condition of $p = 10$, and a moderate size of selection for VSMSPC was chosen, resulting in the overall best performance under the scenarios we consider. In Table 5, δ_i represents the change in the ith variable; for example, $\delta_1 = \delta_3 = 0.25$ means the shift occurs in the first and the third variables with a shift amount of 0.25. In addition, the bold values represent the best of the considered charts. Table 5 shows that BSPC outperforms VSMSPC, RMSPC, and T^2 in most of the scenarios. Accordingly, BSPC shows the minimum RMI, which demonstrates the superiority of BSPC among the charts under various shift directions.

One of the advantages of the proposed chart is that BSPC is directionally invariant. With the Gaussian error distributions for the measurement and the state (i.e., mean), $\hat{\boldsymbol{\mu}}$ follows a Gaussian distribution asymptotically with the covariance $\mathbf{P}_\infty$. Thus, the chart statistic measures the Mahalanobis distance

TABLE 5. ARL1 and RMI with BSPC, VSMSPC, RMSPC, and T^2.

Shifts	T^2	VSMSPC	RMSPC	BSPC
$\delta_1 = 0.25$	133.54(0.47)	127.49(0.4)	127.75(0.41)	90.79(0)
$\delta_2 = 0.5$	36.47(1.68)	26.22(0.92)	26.07(0.91)	13.62(0)
$\delta_3 = 0.75$	10.67(1.43)	7.17(0.63)	7.5(0.71)	4.4(0)
$\delta_5 = 0.5$	52.16(3.42)	11.81(0)	47.57(3.03)	21.11(0.79)
$\delta_7 = 0.25$	117.03(0.65)	108.85(0.53)	97.97(0.38)	71.03(0)
$\delta_9 = 0.75$	10.72(1.43)	6.96(0.58)	7.59(0.72)	4.42(0)
$\delta_1 = \delta_3 = 0.25$	84.05(1.06)	78.13(0.91)	63.38(0.55)	40.88(0)
$\delta_1 = \delta_5 = 0.5$	21.88(1.72)	19.01(1.37)	19.93(1.48)	8.03(0)
$\delta_1 = \delta_7 = 0.75$	3.97(0.7)	3.19(0.36)	2.69(0.15)	2.34(0)
$\delta_1 = \delta_9 = 0.5$	16.04(1.64)	13.36(1.2)	12.8(1.11)	6.07(0)
$\delta_2 = \delta_4 = 0.25$	75.09(1.17)	67.44(0.95)	52.05(0.5)	34.65(0)
$\delta_3 = \delta_8 = 0.5$	20.68(1.73)	20.52(1.71)	17.04(1.25)	7.56(0)
$\delta_3 = \delta_9 = 0.75$	3.27(0.56)	2.75(0.31)	2.32(0.1)	2.1(0)
$\delta_1 = \delta_3 = \delta_7 = 0.25$	56.6(1.39)	47.09(0.99)	33.2(0.4)	23.71(0)
$\delta_2 = \delta_4 = \delta_8 = 0.5$	6.76(1.11)	6.33(0.98)	3.94(0.23)	3.2(0)
$\delta_4 = \delta_5 = \delta_{10} = 0.75$	11.28(1.51)	14.79(2.29)	11.73(1.61)	4.5(0)
$\delta_1 = \delta_2 = \delta_4 = \delta_5 = 0.25$	79.82(1.08)	90.13(1.35)	81.12(1.12)	38.33(0)
$\delta_3 = \delta_4 = \delta_6 = \delta_7 = 0.5$	10.02(1.39)	14.65(2.5)	9.09(1.17)	4.18(0)
$\delta_3 = \delta_5 = \delta_7 = \delta_9 = 0.75$	1.37(0.2)	1.49(0.31)	1.14(0)	1.29(0.12)
$\delta_1 = \delta_2 = \delta_3 = \delta_5 = \delta_7 = 0.25$	65.05(1.27)	62.94(1.19)	52.42(0.83)	28.68(0)
$\delta_2 = \delta_3 = \delta_4 = \delta_8 = \delta_{10} = 0.5$	7.76(1.22)	8.19(1.35)	5.29(0.52)	3.49(0)
$\delta_3 = \delta_5 = \delta_6 = \delta_9 = \delta_{10} = 0.75$	1.88(0.22)	2.05(0.33)	1.54(0)	1.57(0.02)
$\delta_1 = \delta_3 = \delta_5 = \delta_7 = \delta_9 = 0.25$	31.62(1.71)	26.21(1.24)	16.05(0.37)	11.68(0)
$\delta_2 = \delta_4 = \delta_6 = \delta_8 = \delta_{10} = 0.5$	3.23(0.62)	3.41(0.71)	2(0)	2.09(0.05)
$\delta_1 = \delta_3 = \delta_5 = \delta_7 = \delta_9 = 0.5$ $\delta_2 = \delta_4 = \delta_6 = \delta_8 = \delta_{10} = 0.25$	29.5(1.77)	26.28(1.47)	16.03(0.51)	10.64(0)
RMI	1.246	0.984	0.722	0.039

of $\hat{\boldsymbol{\mu}}$ with a fixed covariance matrix, and therefore, we can conjecture that the chart is directionally invariant, just as MEWMA does. In addition, note that the monitoring statistic Q does not follow a χ^2 distribution because $\hat{\boldsymbol{\mu}}_t$ is not i.i.d with respect to t. In the next experiment, we consider several different shift directions with the same noncentrality for out-of-control signals to numerically observe the directional invariance in the simulation. Specifically, we conducted three scenarios, namely $\|\boldsymbol{\mu}_1\|_0 = 2$, 5, and 10 for Cases 1, 2, and 3, respectively. The dimension is set to $p = 10$, and δ represents noncentrality in Table 6. The results show that the ARL1 values were statistically identical among the cases. We conducted more simulations in different settings of p and shift directions—not shown in this paper—but we can deduce the same conclusion.

TABLE 6. Directional invariance of BSPC ($p = 10$, $\|\mu_1\|_0 = 2$, 5, 10 for Cases 1, 2, and 3).

δ	Case 1	Case 2	Case 3
0.5	128.91	128.44	128.66
1.0	47.88	48.11	48.48
1.5	17.37	17.44	17.29
2.0	7.58	7.37	7.53
2.5	4.15	4.09	4.12
3.0	2.69	2.74	2.71
3.5	2.02	2.04	2.00
4.0	1.63	1.62	1.63
4.5	1.36	1.37	1.36
5.0	1.19	1.20	1.20

B. TRACKING MEAN

Statistical process monitoring sequentially tests the hypotheses $H_0 : \boldsymbol{\mu} = \boldsymbol{\mu}_0$ and $H_1 : \boldsymbol{\mu} = \boldsymbol{\mu}_1$, where $\boldsymbol{\mu}_1$ is usually a sudden jump at a certain point and remains unchanged over the sampling period once it occurs. In many manufacturing processes and service processes, processes may go beyond normal conditions in different ways, as discussed in Section 1. In this section, we consider several patterns of out-of-control signals, including a sudden jump, sigmoid, oscillating, and multiple jumps. Moreover, we attempt to interpret the chart from a different angle rather than focusing only on the out-of-control ARL. The idea of the proposed method is to maximize the posterior probability at every sampling point based on the rationale that the estimation with the past means and

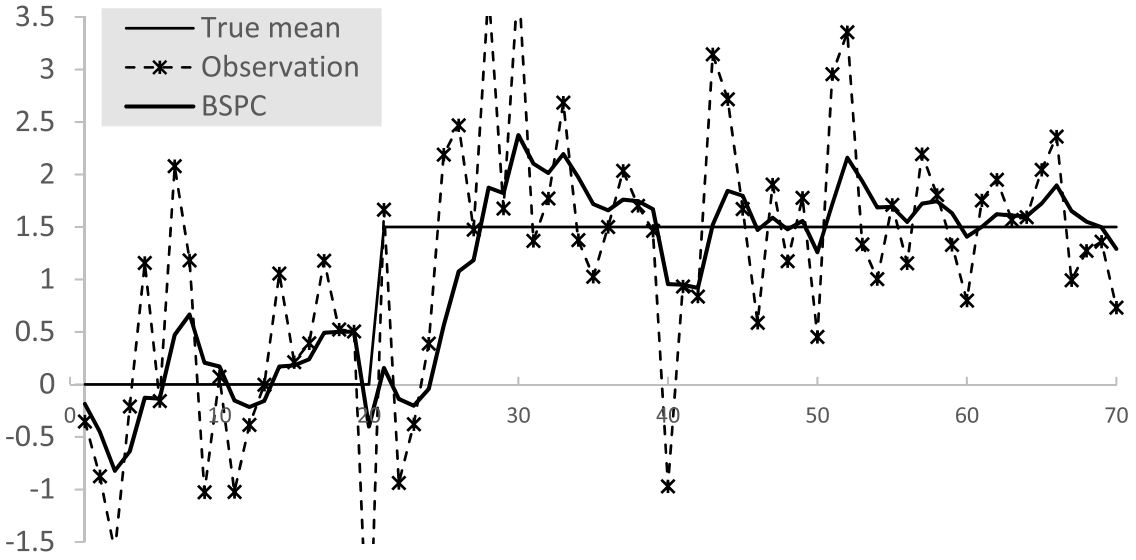

FIGURE 3. A sample path of BSPC with a constant (sudden jump) pattern.

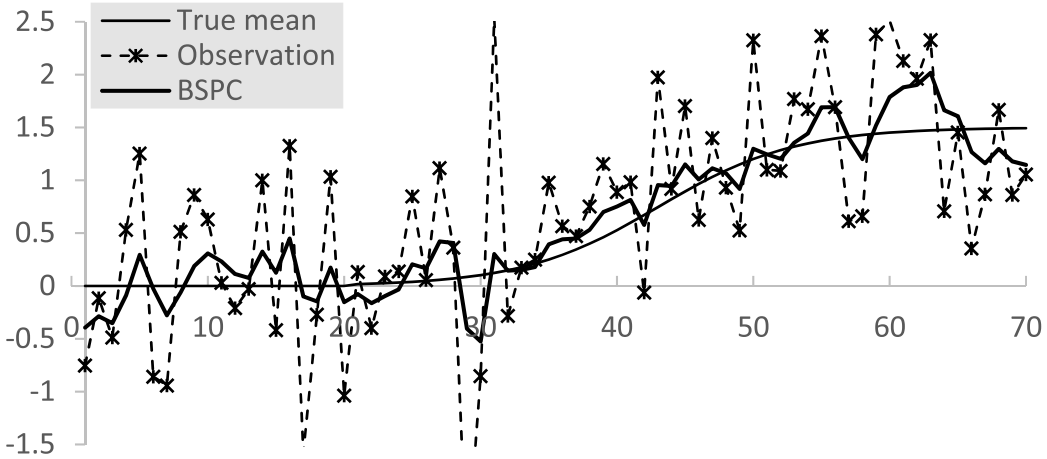

FIGURE 4. A sample path of BSPC with a sigmoid pattern.

observations would support the decision for the current sample. Thus, it is worthwhile to see how accurately the mean is estimated in addition to the ARL performance. One of the measures is the mean squared error (MSE) between the actual and estimated means. The MSE can be calculated as

$$\frac{1}{NT}\sum_{n}^{N}\sum_{t=1}^{T}\left\|\boldsymbol{\mu}_{1,t}^{(n)}-\hat{\boldsymbol{\mu}}_{t}^{(n)}\right\|_{2}^{2}$$

where T is the sampling period and $\boldsymbol{\mu}_{1,t}^{(n)}$ and $\hat{\boldsymbol{\mu}}_{t}^{(n)}$ are the actual and estimated means, respectively, at time t in nth replication. We conducted $N = 1000$ runs to obtain the average squared errors in replications. Regarding the sampling period T, we set $T = 70$ for illustration, and we assume that the process is in-control for the first 20 samples. The experiment was conducted with $p = 25$, and the shift occurred for five variables, including the first variable. Let $\mu_i(t)$ for $i = 1, \ldots, 5$ be the out-of-control signal of the first variable at sampling time t. The following out-of-control signals are considered.

1) Constant (sudden jump): $\mu_i(t) = \frac{0.5}{\sqrt{\mathbf{e}^T\boldsymbol{\Sigma}^{-1}\mathbf{e}}}$, where $\mathbf{e}$ is an elementary vector for which the first five elements are one and the remaining elements are zero (i.e., non-centrality is 0.5)
2) Sigmoid pattern:

$$\mu_i(t) = \frac{1.5}{1+5e^{-0.2(t-35)}}$$

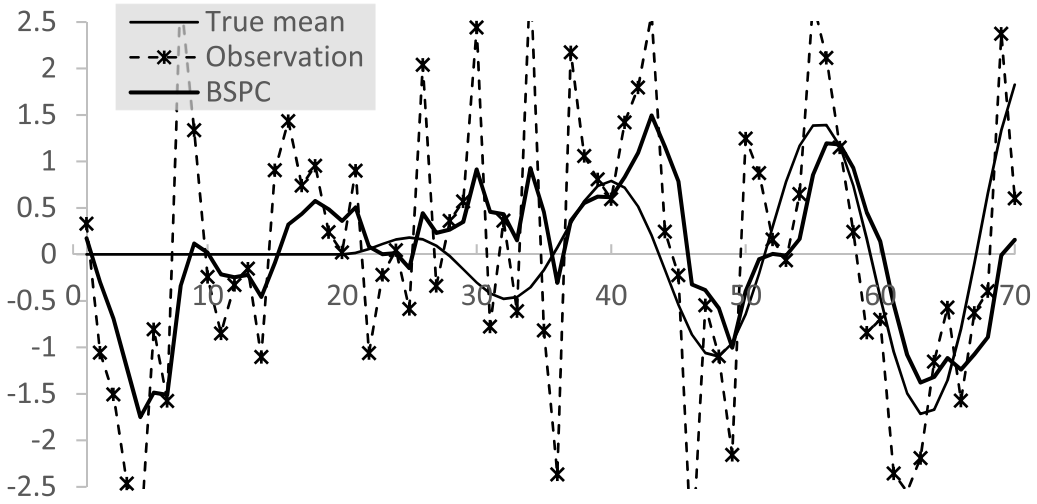

FIGURE 5. A sample path of BSPC with an oscillating pattern.

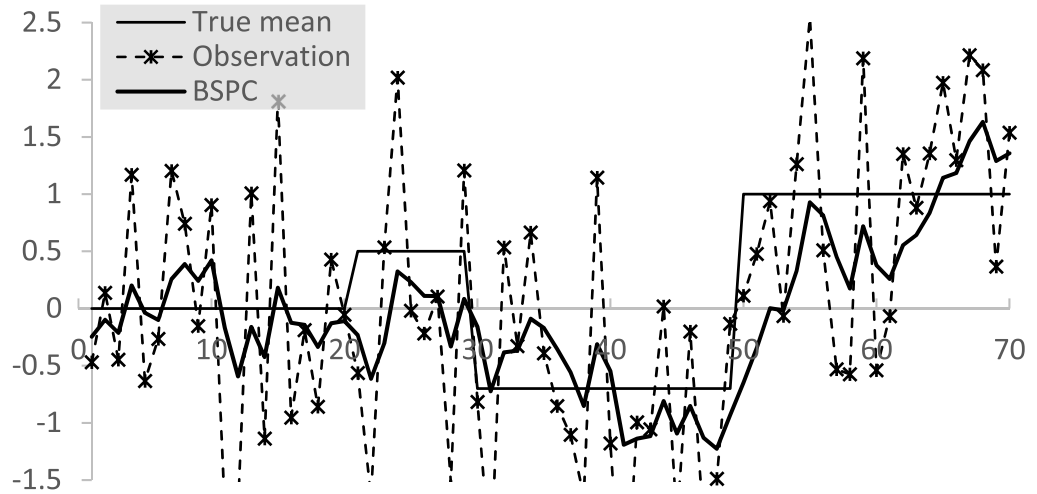

FIGURE 6. A sample path of BSPC with a multiple-jump pattern.

3) Oscillating pattern:

$$\mu_i(t) = 0.04\,(t-20)\sin 0.4\,(t-20)$$

4) Multiple jumps:

$$\mu_i(t) = \begin{cases} 0 & t \le 20 \\ 0.5 & 20 < t \le 30 \\ -0.7 & 30 < t \le 50 \\ 1.0 & t > 50 \end{cases}$$

In addition to the MSE, we also mark the first detection in each replication and calculate the average run length. In this case, we ignore the alarm that the chart triggers in the first 20 in-control samples. Moreover, we set the run length to 50, which is the number of out-of-control samples, if the chart does not detect the out-of-control signal within a replication.

Table 7 presents the MSE and ARL1 for the four cases considered, and Figures 3, 4, 5, and 6 illustrate sample paths for each pattern, where we plot only the first variable. In the figures, the solid and bold lines represent the true mean ($\mu_{1,1}(t)$) and the estimated mean through Bayesian update (BSPC, $\hat{\mu}_{1,t}$), respectively. A dotted line with an asterisk represents the observation, that is, T^2 as the measurement $\mathbf{x}_t$ is the best estimate at each sampling time.

From Figures 3–6, it is clear that the estimated mean through Bayesian update tracks the true mean well even after the process is changed, while the observations fluctuate significantly. Accordingly, the results of MSE and ARL_1 in Table 7 demonstrate the superior performance of the proposed chart to that of the conventional T^2 chart, both in tracking the mean and in detecting the change in the process.

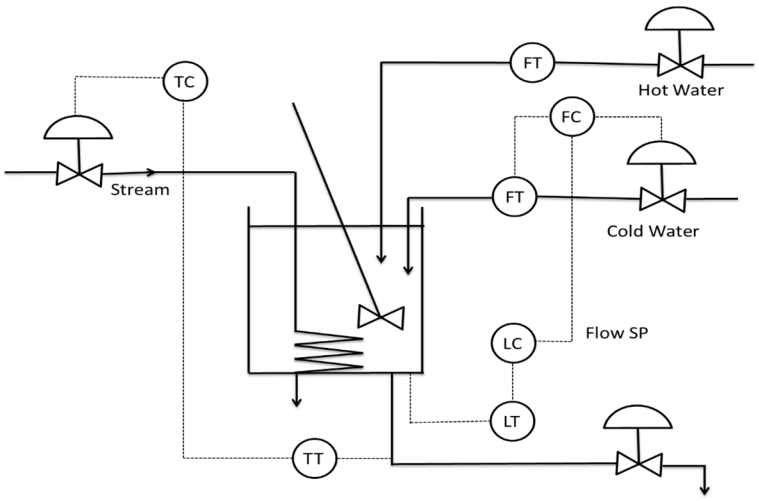

FIGURE 7. Continuous stirred tank heater [41].

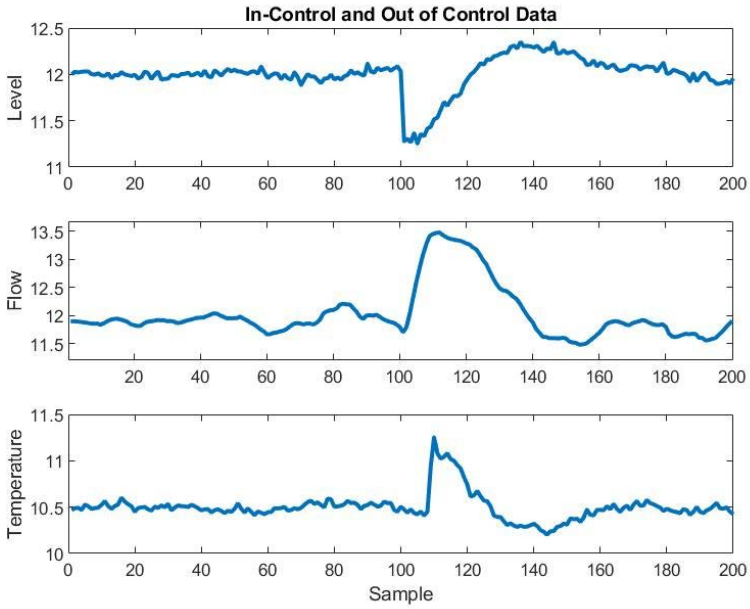

FIGURE 8. In-control and out-of-control data.

IV. CASE STUDY: CONTINUOUS STIRRED TANK HEATER

In this section, we apply the proposed chart to an industrial application that was introduced by [46]. In a tank heater, hot and cold water were mixed inside the tank, and the mixed water was heated using a heating coil, as shown in Figure 7. Finally, the mixed heated water was drained from the tank through a long pipe. The instruments used to monitor the plant are the steam temperature (TC), thermocouple temperature (TT), cold water flow (FC), heating flow (FT), level controller (LC), and heating level (LT). Cold water and hot water enter the plant at a pressure of 60–80 psi and the steam supply heats the mixed water. The liquid level was controlled by a valve on the inlet water pipe, and the outlet flow rate could be adjusted using the valve on the outlet pipe. In addition, the steam coil in the tank had a control valve on the steam line to adjust the heat.

The main aim of the continuous stirred tank heater is to maintain the same temperature in the tank and the outflow while maintaining the volume of the water in the tank at the desired value. Thus, it is reasonable to monitor the temperature in the tank, outflow, and volume as quality characteristics. The tank is equipped with level and outlet flow sensors that measure the water level in the tank (i.e., volume, m^3/s), temperature (°C), and water flow rates (mA). The measurements were obtained using a differential pressure instrument

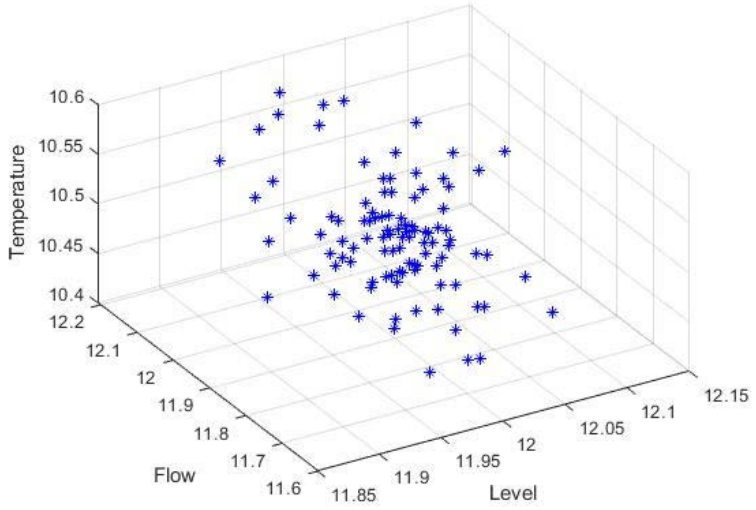

FIGURE 9. Three-dimensional plot of normal operating data.

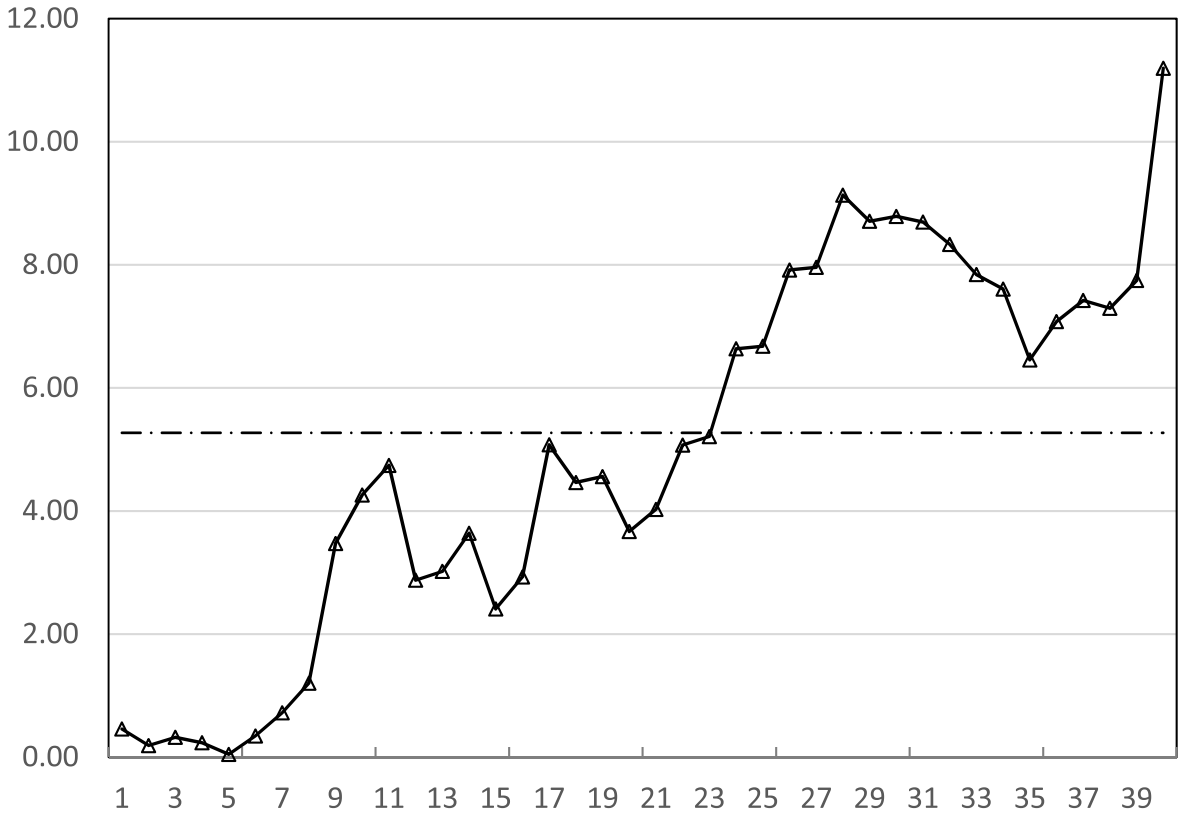

FIGURE 10. An illustration of BSPC in the continuous stirred tank heater.

and a thermocouple inserted into the outflow pipe. Under the normal operating mode of the process, the cold-water flow and level measurements were 12 mA and 12 m^3/s, respectively, and the desired temperature of the water in the tank was 10.5°C [47].

There is a controller that adjusts the setting of the level measurement subsystem and cold-water valve position, called the proportional integral controller (PI). The process continues operating as normal while the PI functions properly and goes out to control if there is any damage or

TABLE 7. MSE and ARL1 of BSPC and T^2 for different patterns of out-of-control signals.

	MSE		ARL1	
	BSPC	T^2	BSPC	T^2
Constant	4.12	25.02	4.96	36.54
Sigmoid	4.67	24.96	14.59	43.17
Oscillation	4.70	25.02	15.91	43.54
Multi-jumps	4.41	25.01	12.71	42.90

disturbance in the controller. The sample data paths shown in Figure 8 present in-control data for the first 100 samples and out-of-control data when the disturbance in the PI is added to the 101st sample. The 3-dimensional plot of the in-control data showing the correlation structure is shown in Figure 9.

As shown in Figure 8, the process appears with white noise in the in-control process, while it shows significantly temporally correlated measurements once the process goes out of control. For illustrative purposes, we plot the successive BSPC monitoring statistics for 20 in-control samples (81st–100th points in the dataset) and another 20 out-of-control samples (101st–120th points) sequentially in Figure 10. The bold line with a triangle mark represents the BSPC monitoring statistics, and the dashed line represents the control limit of 5.27, which was obtained from the 100 in-control samples. The chart triggers alarms at the 23rd observation and keeps it above the control limit after the first alarm.

V. CONCLUDING REMARKS AND FUTURE RESEARCH

In this study, we apply a Bayesian approach to the monitoring of high-dimensional and high-speed monitoring processes. The main contributions of the proposed method can be summarized as follows. First, the proposed chart computes the estimated mean at every sampling point based on the stochastic model, which enables the monitoring statistic to be efficient in many applications where the measurements could be temporally correlated when the process changes. Even when the underlying process is not autocorrelated, consideration of stochastic behavior in charting is beneficial because of the possible autocorrelation in high-speed monitoring processes. In addition, the out-of-control pattern in many manufacturing and service processes is unknown, and the process may change over time. Thus, the proposed method appropriately captures the behavior of the process in both in-control and out-of-control situations.

Second, the proposed method is computationally inexpensive. Whereas many high-dimensional processes aiming charts are computationally heavy, which makes them impractical in real process monitoring, BSPC has a closed form of process parameter estimation, which makes the practical implementation of monitoring highly convenient. In addition to SPC perspectives, the chart provides insight by estimating the process mean sequentially. Moreover, the directionally invariant property of the proposed chart guarantees simplicity under various situations with correlated covariates.

Through various simulation studies and a real-life application, we demonstrate the superiority of the proposed BSPC in high-dimensional and high-speed monitoring processes. Moreover, a simple extension by replacing the measurement with an EWMA-transformed measurement would also be attractive when the process change is expected to be small based on engineering knowledge and experience. Although the proposed method generally performs well under various process scenarios, it can be tuned more appropriately using engineering knowledge. For example, the state transition matrix, autocorrelation parameters, and moving errors in a specific process can be properly determined, which paves the way for future research.

One of the key points in the BSPC procedure is updating the covariance of the mean. Thus, future research should be conducted to monitor process variability as well as the mean. A large body of literature deals with variability monitoring [48], [49], [50], [51], where the estimation of the covariance matrix is the key to the methods. In addition, the estimation procedures are mostly computationally expensive, whereas the propagation of the covariance in the proposed charting procedure is obtained relatively simply as a recursive form, as shown in (13). Thus, it will be interesting to develop a chart to monitor process variability using the updated covariance matrix.

Another interesting research topic is to consider any special settings in high-dimensional processes. Although BSPC generally performs well in most settings, including sparsity cases, the method can narrow a case down to a specific high-dimensional process with expected sparse changes. For example, the error distribution of the process mean can be a sparsity-advocated distribution rather than a Gaussian distribution as shown in [33], so that the distribution would represent the sparse change in the mean more appropriately than the generalized BSPC. In this case, however, updating the mean and covariance may not be computationally easy, making it challenging to monitor high-dimensional processes. Thus, [33] developed an algorithmic procedure to estimate the sparse mean and propagated covariance matrix in such a case. As such, in other special settings, the error distribution can be specifically determined to make the methodology suitable to the process setting.

Although the proposed method applies the Bayesian update to estimate the quality characteristics, other popular algorithms such as meta-heuristics, e.g., data envelopment analysis, non-dominated sorting genetic algorithm, grey wolf optimizer, and so on can also be used to obtain the optimal parameters with given in-control and out-of-control circumstances. Such optimizers are expected to be beneficial in quality control and monitoring aspects, e.g., cost of sampling, run length, and lessening false alarms.

Not to mention, when a small shift in process change is expected, CUSUM can also be applied instead of EWMA. It will be interesting to see if CUSUM is comparable to EWMA in this Bayesian context.

REFERENCES

[1] R. B. Crosier, "Multivariate generalizations of cumulative sum quality-control schemes," *Technometrics*, vol. 30, no. 3, pp. 291–303, Aug. 1988.

[2] C. A. Lowry, W. H. Woodall, C. W. Champ, and S. E. Rigdon, "A multivariate exponentially weighted moving average control chart," *Technometrics*, vol. 34, no. 1, pp. 46–53, 1992.

[3] K. Wang and W. Jiang, "High-dimensional process monitoring and fault isolation via variable selection," *J. Quality Technol.*, vol. 41, no. 3, pp. 247–258, Jul. 2009.

[4] J. Friedman, T. Hastie, and R. Tibshirani, *The Elements of Statistical Learning* (Springer Series in Statistics), vol. 1, no. 10. New York, NY, USA: Springer, 2001.

[5] M. L. Shyu, S. C. Chen, K. Sarinnapakorn, and L.-W. Chang, "A novel anomaly detection scheme based on principal component classifier," in *Proc. IEEE Found. New Directions Data Mining*, Melbourne, FL, USA, 2003, pp. 171–179.

[6] W. Wang and R. Battiti, "Identifying intrusions in computer networks with principal component analysis," in *Proc. 1st Int. Conf. Availability, Rel. Secur. (ARES)*, 2006, pp. 1–8.

[7] W. Wang, X. Guan, and X. Zhang, "A novel intrusion detection method based on principal component analysis in computer security," in *Proc. Int. Symp. Neural Netw.* Berlin, German: Springer, 2004, pp. 657–662.

[8] S. Kim, M. K. Jeong, and E. A. Elsayed, "A penalized likelihood-based quality monitoring via L_2-norm regularization for high-dimensional processes," *J. Quality Technol.*, vol. 52, no. 3, pp. 265–280, Jul. 2020.

[9] W. Jiang, K. Wang, and F. Tsung, "A variable-selection-based multivariate EWMA chart for process monitoring and diagnosis," *J. Quality Technol.*, vol. 44, no. 3, pp. 209–230, Jul. 2012.

[10] C. Zou and P. Qiu, "Multivariate statistical process control using LASSO," *J. Amer. Statist. Assoc.*, vol. 104, no. 488, pp. 1586–1596, Dec. 2009.

[11] G. Capizzi and G. Masarotto, "A least angle regression control chart for multidimensional data," *Technometrics*, vol. 53, no. 3, pp. 285–296, Aug. 2011.

[12] G. M. Abdella, K. N. Al-Khalifa, S. Kim, M. K. Jeong, E. A. Elsayed, and A. M. Hamouda, "Variable selection-based multivariate cumulative sum control chart," *Quality Rel. Eng. Int.*, vol. 33, no. 3, pp. 565–578, Apr. 2017.

[13] J. J. Downs and E. F. Vogel, "A plant-wide industrial process control problem," *Comput. Chem. Eng.*, vol. 17, no. 3, pp. 245–255, Mar. 1993.

[14] A. Raich and A. Çinar, "Statistical process monitoring and disturbance diagnosis in multivariable continuous processes," *AIChE J.*, vol. 42, no. 4, pp. 995–1009, Apr. 1996.

[15] R. L. Mason, N. D. Tracy, and J. C. Young, "Decomposition of T^2 for multivariate control chart interpretation," *J. Quality Technol.*, vol. 27, no. 2, pp. 99–108, 1995.

[16] J. Kim, M. K. Jeong, E. A. Elsayed, K. N. Al-Khalifa, and A. M. S. Hamouda, "An adaptive step-down procedure for fault variable identification," *Int. J. Prod. Res.*, vol. 54, no. 11, pp. 3187–3200, 2016.

[17] F. Naderkhani and V. Makis, "Economic design of multivariate Bayesian control chart with two sampling intervals," *Int. J. Prod. Econ.*, vol. 174, pp. 29–42, Apr. 2016.

[18] V. Makis, "Multivariate Bayesian control chart," *Oper. Res.*, vol. 56, no. 2, pp. 487–496, 2008.

[19] G. Tagaras and Y. Nikolaidis, "Comparing the effectiveness of various Bayesian X control charts," *Oper. Res.*, vol. 50, no. 5, pp. 878–888, Oct. 2002.

[20] C. Duan, V. Makis, and C. Deng, "A two-level Bayesian early fault detection for mechanical equipment subject to dependent failure modes," *Rel. Eng. Syst. Saf.*, vol. 193, Jan. 2020, Art. no. 106676.

[21] M. Tavakoli and R. Pourtaheri, "Economic and economic-statistical design of multivariate Bayesian control chart with variable sampling intervals," *Pakistan J. Statist. Operation Res.*, vol. 16, no. 4, pp. 737–750, Dec. 2020.

[22] F. Naderkhani, "Time to signal distribution of multivariate Bayesian control chart with dual sampling scheme," *Int. J. Prod. Res.*, p. 124, Nov. 2021, doi: 10.1164/rccm.168.7.818.

[23] Y. Wu and W. B. Wu, "Sequential detection of common transient signals in high dimensional data stream," *Nav. Res. Logistics*, vol. 69, no. 4, pp. 640–653, 2021.

[24] Y. Hou, B. He, X. Zhang, Y. Chen, and Q. Yang, "A new Bayesian scheme for self-starting process mean monitoring," *Qual. Technol. Quant. Manage.*, vol. 17, no. 6, pp. 661–684, Nov. 2020.

[25] D. W. Apley, "Posterior distribution charts: A Bayesian approach for graphically exploring a process mean," *Technometrics*, vol. 54, no. 3, pp. 279–293, Aug. 2012.

[26] P. Tsiamyrtzis and D. M. Hawkins, "A Bayesian scheme to detect changes in the mean of a short-run process," *Technometrics*, vol. 47, no. 4, pp. 446–456, Nov. 2005.

[27] P. Tsiamyrtzis and D. M. Hawkins, "Bayesian startup phase mean monitoring of an autocorrelated process that is subject to random sized jumps," *Technometrics*, vol. 52, no. 4, pp. 438–452, 2010.

[28] P. W. Woodward and J. C. Naylor, "An application of Bayesian methods in SPC," *J. Roy. Stat. Soc. D, Statistician*, vol. 42, no. 4, pp. 461–469, 1993.

[29] W. H. Woodall and D. C. Montgomery, "Some current directions in the theory and application of statistical process monitoring," *J. Quality Technol.*, vol. 46, no. 1, pp. 78–94, 2014.

[30] R. Pan and S. E. Rigdon, "A Bayesian approach to change point estimation in multivariate SPC," *J. Quality Technol.*, vol. 44, no. 3, pp. 231–248, 2012.

[31] M. H. Tan and J. Shi, "A Bayesian approach for interpreting mean shifts in multivariate quality control," *Technometrics*, vol. 54, no. 3, pp. 294–307, 2012.

[32] C. Duan, "Dynamic Bayesian monitoring and detection for partially observable machines under multivariate observations," *Mech. Syst. Signal Process.*, vol. 158, Sep. 2021, Art. no. 107714.

[33] S. Kim and M. Turkoz, "Bayesian sequential update for monitoring and control of high-dimensional processes," *Ann. Oper. Res.*, pp. 1–23, Jul. 2021.

[34] J. Durbin and S. J. Koopman, *Time Series Analysis by State Space Methods*. Oxford, U.K.: Oxford Univ. Press, 2012.

[35] J. Jin and J. Shi, "State space modeling of sheet metal assembly for dimensional control," *J. Manuf. Sci. Eng.*, vol. 121, no. 4, pp. 756–762, 1999.

[36] Y. Ding, D. Ceglarek, and J. Shi, "Fault diagnosis of multistage manufacturing processes by using state space approach," *J. Manuf. Sci. Eng.*, vol. 124, no. 2, pp. 313–322, 2002.

[37] Q. Huang and J. Shi, "Variation transmission analysis and diagnosis of multi-operational machining processes," *IIE Trans.*, vol. 36, no. 9, pp. 807–815, 2004.

[38] J. E. Jarrett and X. Pan, "Monitoring variability and analyzing multivariate autocorrelated processes," *J. Appl. Statist.*, vol. 34, no. 4, pp. 459–469, May 2007.

[39] J. Shi and S. Zhou, "Quality control and improvement for multistage systems: A survey," *IIE Trans.*, vol. 41, no. 9, pp. 744–753, 2009.

[40] J. Kim, M. K. Jeong, and E. A. Elsayed, "Monitoring multistage processes with autocorrelated observations," *Int. J. Prod. Res.*, vol. 55, no. 8, pp. 2385–2396, 2017.

[41] A. S. Charles, A. Balavoine, and C. J. Rozell, "Dynamic filtering of time-varying sparse signals via L_1 minimization," *IEEE Trans. Signal Process.*, vol. 64, no. 21, pp. 5644–5656, Nov. 2016.

[42] L. Bao, K. Wang, and R. Jin, "A hierarchical model for characterising spatial wafer variations," *Int. J. Prod. Res.*, vol. 52, no. 6, pp. 1827–1842, 2014.

[43] K. Liu, Y. Mei, and J. Shi, "An adaptive sampling strategy for online high-dimensional process monitoring," *Technometrics*, vol. 57, no. 3, pp. 305–319, Jul. 2015.

[44] K. Wang, W. Jiang, and B. Li, "A spatial variable selection method for monitoring product surface," *Int. J. Prod. Res.*, vol. 54, no. 14, pp. 4161–4181, 2016.

[45] S. Kim, M. K. Jeong, and E. A. Elsayed, "Generalized smoothing parameters of a multivariate EWMA control chart," *IISE Trans.*, vol. 49, no. 1, pp. 58–69, 2017.

[46] N. F. Thornhill, S. C. Patwardhan, and S. L. Shah, "A continuous stirred tank heater simulation model with applications," *J. Process Control*, vol. 18, nos. 3–4, pp. 347–360, 2008.

[47] S. Sehgal and V. Acharya, "Design of PI controller for continuous stirred tank heater process," in *Proc. IEEE Students' Conf. Elect., Electron. Comput. Sci.*, Mar. 2014, pp. 1–5.

[48] J. Kim, G. M. Abdella, S. Kim, K. N. Al-Khalifa, and A. M. Hamouda, "Control charts for variability monitoring in high-dimensional processes," *Comput. Ind. Eng.*, vol. 130, no. 2, pp. 309–316, 2019.
[49] B. Li, K. Wang, and A. B. Yeh, "Monitoring the covariance matrix via penalized likelihood estimation," *IIE Trans.*, vol. 45, no. 2, pp. 132–146, 2013.
[50] D. M. Hawkins and E. M. Maboudou-Tchao, "Multivariate exponentially weighted moving covariance matrix," *Technometrics*, vol. 50, no. 2, pp. 155–166, May 2008.
[51] F. B. Alt, "Multivariate quality control," *Encyclopedia Stat. Sci.*, vol. 6, pp. 110–122, Jan. 1985.

SANGAHN KIM received the Ph.D. degree from the Department of Industrial and Systems Engineering, Rutgers University, USA. He is currently an Assistant Professor with the Department of Business Analytics and Actuarial Science, Siena College, NY, USA. His research interests include data analytics, process modeling and monitoring, stochastic process, reliability engineering, statistical learning, and machine learning. He was a recipient of the Richard A. Freund International Scholarship by American Society for Quality (ASQ), in 2016.

MEHMET TURKOZ received the M.S. degree in operations research from Rutgers University, USA, in 2012, where he received the Ph.D. degree from the Department of Industrial and Systems Engineering, in 2018. He was an Assistant Professor of professional practice at the Department of Management Science and Information Systems, Rutgers Business School, from September 2018 to August 2020. He is currently an Assistant Professor with the Department of Management, Marketing, and Professional Sales, William Paterson University. His research interests include business analytics, machine learning, statistical process modeling and monitoring, data mining, and operations research.

JUNG WOO BAEK received the Ph.D. degree from the Department of Industrial Engineering, Sungkyunkwan University, South Korea, in 2010. He is an Associate Professor with the Department of Industrial Engineering, Chosun University, South Korea. His research interests include queueing theory, stochastic modeling and analysis, inventory control, telecommunication modeling, and operations research.